

Screening and Identification of Potential Key Biomarkers in Psoriasis : Evidence From Bioinformatic Analysis

Yang Yang

Shanghai Skin Diseases Hospital

Shaoqiong Xie

Shanghai Skin Diseases Hospital

Jiajing Lu

Shanghai Skin Diseases Hospital

Suwei Tang (✉ tangsuwei1115@126.com)

: Shanghai Skin Diseases Hospital <https://orcid.org/0000-0002-3590-6027>

Research

Keywords: psoriasis, bioinformatic analysis, CXCL8, molecular mechanism

Posted Date: May 24th, 2021

DOI: <https://doi.org/10.21203/rs.3.rs-516404/v1>

License:  This work is licensed under a Creative Commons Attribution 4.0 International License.

[Read Full License](#)

Abstract

Background: Psoriasis is a chronic and prevalent skin condition brought on by various genetic and external factors. Till date, there is no cure for this disease. It is, therefore, crucial to examine the underlying mechanisms leading up to psoriasis. The goal of our study was to explore the mechanistic pathways involved in the molecular pathogenesis of psoriasis.

Methods: Using Gene Expression Omnibus (GEO), we performed an extensive analysis of the transcript expression profile in psoriasis patients. The datasets GSE13355, GSE30999, and GSE106992, containing 239 pairs of normal and psoriatic skin samples were arbitrarily assigned to two non-overlapping cohorts for cross-validated differential gene expression analysis. The gene ontology (GO) and Kyoto Encyclopedia of Genes and Genomes (KEGG) enrichment and gene set enrichment analysis (GSEA) were employed for interpretation, visualization, and unified recognition. The STRING database was used to construct the protein–protein interaction (PPI) network and the hub genes were established using Cytoscape. Additionally, both differentially regulated genes and functional likeness of hub genes were further examined in terms of gene activation and functional outcome. The correlation between normal tissue and infiltrating immune cells was analyzed by CIBERSORT. Moreover, ROC analysis was performed to distinguish between skin lesion samples and skin non-lesion samples. In addition, a signaling axis involving lncRNA, miRNA, mRNA, and ceRNA was generated with information from the DE miRNA, DE lncRNA, and DE miRNA-DE mRNA relationship. Lastly, immunohistochemical evaluations were used to analyze the highest expression of single gene in the whole body within the Human Protein Atlas (HPA) database.

Results: The genetic profiles of 239 pairs of normal and lesional skin samples were downloaded from three datasets in the GEO database. PPI network revealed a tight interaction among 197 differentially expressed genes (DEGs). Moreover, gene ontology analyses indicated that psoriasis-related DEGs mostly included viral defense genes, type I interferon axis, and its corresponding cellular responses. The Kyoto encyclopedia of genes and the DEGs enrichment analysis showed involvement of the NOD-like receptor signaling network, cytokine-cytokine receptor binding, and IL-17 signaling axis in psoriasis verses non-psoriatic tissues. GSEA analysis demonstrated that CXCL8 was only enriched in the "complement characteristic" pathway. ROC curves indicated that CXCL8 expression was highly effective in classifying both lesional and non-lesional skin samples (with AUC 0.941, 0.935, and 0.794 for GSE13355, GSE30999, and GSE 106992). Furthermore, CIBERSORT database indicated that CXCL8 was correlated to 22 types of infiltrating immune cells. In addition, 6 miRNAs were predicted to be related to CXCL8, including hsa-miR-1294, hsa-miR-140-3p, hsa-miR-185-5p, hsa-miR-4306, hsa-miR-4644, and hsa-miR-493-5p. Lastly, immunohistochemical analysis showed that CXCL8 was most widely distributed in lymphoid tissues.

Conclusions: Based on our analysis, CXCL8 plays a key role in psoriatic development. Our comprehensive bioinformatics analysis of the GEO data provided new insights into the exploration of molecular mechanisms while searching for highly efficient therapeutic targets for treating psoriasis.

Introduction

Psoriasis is a chronic autoimmune skin disorder manifested by scaly erythema and regulated by genetic and environmental agents[1]. Although psoriasis poses no threat to life, it can present serious mental and economic burden to patients. Fortunately, with better understanding of psoriasis[2-3], an increasing number of therapies have emerged. The mainstream psoriatic therapy includes systemic application of retinoic acid, immunosuppressant, cyclosporine, biological agents, external use of glucocorticoid, retinoic acid drugs, and so on. However, the adverse reactions are serious. Due to the unclear etiology and complex pathogenesis of psoriasis, it still remains incurable. Hence, there is great urgency in the comprehension of molecular networks involved in psoriasis to enhance the quality of psoriatic care.

Psoriasis is mediated by polygenic inheritance T cells. The excessive activation of immune cells is caused by a variety of pathogenic factors. At present, multiple new drugs are available for the management of psoriasis. The biological agents used for psoriasis therapy in China are anti-TNF- α , anti-IL17A, anti-IL12/23, and anti-IL23. Anti-TNF- α was the first commercially available biological agent for psoriasis, and it includes Etanercept, Adalimumab, and Infliximab. Among them, Etanercept sequesters serum TNF- α , which limits its activity, and produces an anti-inflammatory response[4]. Likewise, Adalimumab also binds to TNF - α and blocks its interaction with the TNF receptor on the surface of p55 and p75 cells, thereby reducing inflammation. Lastly, Infliximab is a human mouse chimeric monoclonal antibody, which strongly sequesters both soluble and transmembrane forms of TNF - α , thereby making them inactive[5]. According to reports, Adalimumab and Infliximab fared better than Etanercept in controlling psoriatic skin lesions. Moreover, the onset speed of Adalimumab and Infliximab remained slower than that of anti-IL17A [6]. The anti-IL17A drugs prevalent in China are Scuchizumab and Iqizumab. Both drugs have similar efficacy in psoriatic lesion resolution and have a better rate of improvement in PASI than monoclonal antibodies[7-9]. Despite the presence of multiple psoriatic drugs, there is still potential for advancements, especially in terms of making the drugs affordable and in reducing double infection risk. Hence, understanding the intricate details of psoriatic pathogenesis will add value to the future of psoriatic care.

Multiple studies have revealed that a variety of chemokines and receptors mediate pathogenesis of psoriasis [10-11], and the CXC family plays an important role. Some chemokines stimulate the chemotactic induction of inflammatory T cells (such as CXCL10, CXCL16) and neutrophils (such as CXCL1 and CXCL5) during psoriasis. The chemokine receptors involved during this process include: T cells: CXCR1, CXCR2, CXCL3, CXCL10, and CXCL16; and neutrophils: CXCL1, CXCL5, CXCR3, and CXCR6 [12]. There is emerging evidence that CXCL10 and its receptor CXCR3 are expressed in keratinocytes and dermis of plaque psoriasis patients. Moreover, upon effective treatment, CXCL10 levels diminish, whereas CXCL10 levels remain high in the serum of early psoriatic patients, but reduce in serum of patient with longer duration of the disease [13]. Multiple studies have revealed that the infiltrating leukocytes in psoriatic lesions strongly express CCR4 and CXCR3, whereas, in the dermis, the ligands CCL17, CCL22, and CXCL9, CXCL10, and CXCL8 are highly expressed. Alternately, others have shown that the CCL2- and CXCL10-related antibodies diminish the expression of these ligands in psoriatic lesions, thereby reducing

severity of psoriasis, as evidenced by the PASI score [14]. CXCL8 is known to regulate neutrophil infiltration, angiogenesis, and keratinocyte proliferation in psoriatic lesions. It is worth mentioning that serum CXCL8 in psoriatic patients remains significantly elevated and is positively correlated with the severity of the disease [15-16]. Nevertheless, the specific function of CXCL8 in psoriatic progression remains unknown and requires further investigation.

Over the past decade, advances in microarray screening and bioinformatics investigations have enabled the genome-wide search for differentially expressed genes (DEGs) and physiological networks linked to specific diseases, including psoriasis. Yet, there have been limitations. For example, a high false-positive incidence was noted in an isolated microarray study. Additionally, differences in microarray procedures, variations in statistical analysis, and limited sample populations may have, in unison, introduced discrepancies in conclusions across studies. Hence, additional extensive examinations are warranted to reliably recognize psoriasis-related DEGs in the search of effective targeted therapy and prognostic biomarkers for psoriasis.

The goal of our work was to analyze DEGs, collected from three microarray datasets from the Gene Expression Omnibus (GEO) database, comparing psoriatic skin to healthy skin. Additionally, we conducted network analyses to further evaluate underlying molecular mechanisms involved in psoriasis. Using the results of our analysis, we established an extensive network of genes and functional pathways involved in psoriasis. Moreover, we demonstrated CXCL8 to be a promising psoriatic biomarker.

Materials And Methods

Data collection and preprocessing

The raw psoriatic gene expression data (cel files), including GSE13355 (58 psoriatic skin specimen verses 64 healthy skin specimen), GSE30999 (82 psoriatic skin specimen verses 82 healthy skin specimen s), and GSE106992 (125 psoriatic skin specimen verses 67 healthy skin specimen), were retrieved from the GEO database (<https://www.ncbi.nlm.nih.gov>)[17]. Simultaneously, the hall marker gene information was obtained from the Molecular Signatures Database (MSigDB) (<https://www.gsea-msigdb.org/gsea/msigdb>)[18]. Lastly, the gene expression data of 33 cancer types were obtained from the UCSC Xena (<http://xena.ucsc.edu/>)[19].

Screening of DEGs

DEG analysis was done with R 3.4.1's (<https://www.r-project.org/>) Affy and Limma package [20-21]. The corresponding plots were made by R and the genes that followed the following criteria were regarded as DEGs: $P \leq 0.05$ and $\log |FC| \geq 1.0$. Finally, we generated Venn charts [22], including an overlap of total, upregulated, and downregulated DEGs from all 3 datasets.

GO and KEGG enrichment analyses of DEGs

Gene Ontology (GO)[23] enrichment analysis and Kyoto encyclopedia of Genes and Genomes (KEGG)[24] functional network analysis were conducted using “clusterProfiler”[25] within R. This allowed us to recognize potential DEG roles and relationships with corresponding diseases. Gene sets carrying a p value ≤ 0.05 was regarded as significant enrichment.

GSEA analysis

The relationship between CXCL8 and functional network genes was analyzed with gene set enrichment analysis (GSEA, v2.2, <http://www.broad.mit.edu/gsea/>)[26]. Furthermore, its association with phenotype was explored with TCGA gene sets that included 33 forms of cancer from MSigDB. The gene sets that showed marked enrichment by genes, based on elevated CXCL8 levels, [false discovery rate (FDR) ≤ 0.05] were defined as enriched gene sets.

Integration of the protein-protein interaction (PPI) network

The PPI network was estimated with the online Search Tool for the Retrieval of Interacting Genes (STRING; <http://string-db.org>)(version 10.0) [27] database and it was formed with the STRING database, with a combined interaction score ≥ 0.4 deemed as significant. Cytoscape (version 3.4.0) was employed for the visualization of potential underlying signaling pathways [28]. Finally, Ggplot2 package[29] was used to generate a bar chart illustrating distribution of relevant genes.

Immune infiltration analysis

CIBERSORT was employed for immune cell infiltration analysis[30] and facilitated the identification of alterations in infiltrating immune cell between psoriatic and healthy skin specimen. The corresponding bubble graph was visualized with ggplot2 package.

Receiver operating characteristic (ROC) curve analysis

ROC curve analysis, conducted with the “pROC” package of R[31], was chosen for determining specificity and sensitivity of the diagnosis[32]. The maximum value of the sum of specificity and sensitivity was set as the threshold for individual hub genes.

Construction of the ceRNA network

The relationship between DElncRNAs and DEmiRNAs were estimated with miRcode[33]. The DEmiRNA-targeted mRNAs were obtained based on starBase[34], miRDB[35], and miRWalk[36]. To be deemed as candidate mRNAs, the mRNAs had to be identified by all data sets and required intersection with DEmRNAs to remove DEmiRNAs-targeted DEmRNAs. Next the lncRNA–miRNA–mRNA ceRNA axis was generated using the DEmiRNA–DElncRNA and DEmiRNA–DEmRNA relationships, and was visualized with the Cytoscape software[28]. Please refer to Figure 11A for a detailed depiction of the lncRNA–miRNA–mRNA ceRNA network analysis. Potential associations between ceRNA levels were analyzed with linear regression.

Immunohistochemical (IHC) analysis of lymph nodes through HPA database

To explore the diagnostic significance of CXCL8, whole-body distribution of this gene (both at the transcript and protein level) was examined using the Human Protein Atlas (HPA, <https://www.proteinatlas.org/>), an open access website providing protein maps within organs, tissues, and cells [37].

Results

Analysis of DEGs

We utilized the Affy and Limma packages to analyze the three GEO data sets. The Venn diagram, consisting of 197 DEGs, from the three data sets, is illustrated in Figure 1A. The DEGs were further analyzed using the STRING database to identify potential links with other DEGs. An interaction network diagram for these genes was additionally generated (Fig. 2A). Figure 2B illustrates each DEG as a node and presents the degrees of each node. Based on this analysis, the degrees of the CXCL8 gene were found to be the largest, suggesting an essential role of CXCL8 in psoriasis. Hence, CXCL8 was selected for further analysis.

Analyzing single gene differences

Next, we separated all samples into a high- or low-expressing group, based on their level of CXCL8 expression, and analyzed the differences between the groups (Figure 3). The GSE13355 data set had 62 high-expressing genes and 62 low-expressing genes. Likewise, the GSE30999 data set had 82 high-expressing genes and 82 low-expressing genes. Lastly, the GSE106992 data set had 96 high- and 96 low-expressing genes. Moreover, the heat map showed a marked difference in CXCL8 levels between the high- and low-expressing groups. Finally, based on the volcano plot, most genes were down-regulated in the GSE13355 and GSE30999 data sets, while the remaining genes were up-regulated in GSE106992.

CXCL8 enrichment analysis

The Venn diagram of 254 low- and high-expressing co-DEGs from the three data sets is shown in Figure 2B. In addition, we performed GO enrichment analysis and KEGG enrichment analysis on these genes (Figure 4). The GO analysis showed that these genes were markedly enriched in the “defense response to virus”, “type I interferon signaling pathway”, and “cell response to type I interferon” categories. Moreover, based on the KEGG analysis, these genes are markedly enriched in the “NOD-like receptor signaling pathway”, “interaction between cytokine and cytokine receptor”, and “IL-17 signaling pathway” categories (Table 1).

GSEA and analysis of pan-cancer pathway

The biological pathways that were significantly altered in the CXCL8 high-expressing versus low-expressing group were determined using GSEA. These pathways were mainly related to the complement-

like network (Figure 5A). To examine CXCL8 pathway enrichment in each cancer type, pan-cancer pathway analysis of CXCL8 was performed (Figure 5B) to identify the distribution pattern of CXCL8 gene in pan-cancer.

Immune infiltration analysis

The immune infiltration analyses of all three data sets were performed separately and the immune cell composition of each sample are displayed in a bar chart. We also analyzed correlation between immune cell expression and differences within them, which are displayed in a heat map and volcano plot respectively. The analytical conclusions from data sets GSE13355, GSE30999, and GSE106992 are provided in Figures 6, 7, and 8 respectively.

ROC analysis

To better elucidate the relationship between CXCL8 expression and classification of diseased verses healthy tissues, we performed ROC analysis of the CXCL8 gene among the 3 data sets (Figure 9). The area under the ROC curves was 0.941 for GSE13355, as shown in Fig. 9A. The area under the ROC curve was 0.935 for GSE30999, as shown in Fig. 9B. The area under the ROC curve was 0.794 for GSE106992, as shown in Fig. 9C.

Constructing the ceRNA network

Integrating starBase, miRDB, and miRWalk, 6 miRNAs, namely, hsa-miR-1294, hsa-miR-140-3p, hsa-miR-185-5p, hsa-miR-4306, hsa-miR-4644, and hsa-miR-493-5p, were predicted to interact with CXCL8 (Figure 10A). StarBase was further used to predict possible lncRNA interactions with any of the 6 six miRNAs (Figure 10C-H). Finally, using these data, a ceRNA network of CXCL8 gene was constructed (Figure 10B).

HIC analysis

The CXCL8 gene was further analyzed, using the HPA database, to obtain CXCL8 gene expression and distribution patterns throughout the human body. We discovered that CXCL8 was most highly expressed within the lymph node. We, thus, selected the lymph node for HIC analysis, and downloaded the HIC map of the CXCL8 gene in the lymph node (Figure 11).

Discussion

Psoriasis is a highly prevalent and chronic inflammatory skin disorder. According to the latest epidemiological survey, the annual incidence rate of psoriasis in European countries is about 0.96 per thousand[38]. This disease is often chronic and recurrent in nature, which offers different degrees of negative impact on the life of patients, involving physiology, psychology, daily life, social contact, family and other aspects. A foreign survey on psoriatic patients revealed that 79% of the patients agreed that the disease had a negative impact on their lives, and 10% of the patients entertained the idea of suicide[39]. Unfortunately, despite the availability of multiple therapeutics for psoriasis, this disease remains

incurable and a vast majority of treated patients experience adverse reactions to psoriatic drugs. As a result, there is great urgency in the development of highly specific and efficient psoriatic biomarkers. Here, we utilized bioinformatics analysis of three separate microarray data sets, involving a total of 265 psoriatic vs. 213 healthy samples, to identify genes specific to the pathogenesis of psoriasis. Among the DEGs studied, CXCL8 showed the largest fold change and is intimately linked to viral defense, type I interferon axis, and its corresponding cellular response. We further delineated the CXCL8 role in psoriasis by assessing its overall expression profile along with evaluating its underlying mechanism of action.

Multiple studies have demonstrated CXCL8 to be an essential cytokine. It often regulates tumor growth, invasion, and neovascularization and can be found in excess in tissues from skin squamous cell carcinoma patients[40]. Earlier reports have also indicated that CXCL8 modulates the formation of psoriasis Munro micro abscess. We, therefore, assessed CXCL8 expression in patients with psoriasis. Given that the role of CXCL8 in psoriasis has not been fully elucidated, we also explored the underlying function of CXCL8 in psoriasis.

Here, we conducted a comprehensive analysis of three microarray data sets to retrieve DEGs involved with psoriasis verses healthy skin specimen. We discovered 187 DEGs in total among the 3 data sets. We further explored interrelationships between DEGs, using GO and KEGG enrichment analyses. Moreover, we conducted analysis with the STRING database to verify the links among the DEGs. 30 DEGs were chosen as hub genes carrying degrees ≥ 20 . Among them, CXCL8 exhibited the largest node degrees with 76, indicating its strong importance in the development and/or progression of psoriasis. Furthermore, using GO enrichment analysis, we demonstrated that alterations in the markedly obvious modules occurred in response to virus, type I interferon axis and its corresponding cellular response. Conversely, using KEGG, it was shown that the DEGs were mainly in the NOD-like receptor axis, interaction between cytokine and cytokine receptor and the IL-17 axis. Multiple studies have reported a strong relation between the IL-17 axis and psoriasis. In fact, IL-17 expression is markedly elevated in the psoriatic skin, compared to healthy skin[41]. It was also shown in keratinocytes that IL-17 stimulated the production of pro-inflammatory cytokines like IL-6 and IL-8, which exacerbated psoriasis[42]. Moreover, topical administration of imiquimod, a Toll-like receptor (TLR) 7/8 ligand and powerful immunologic stimulator, resulted in psoriasis-resembling dermatitis in mice, with simultaneous increases in IL-17A and IL-17F levels[43]. Alternately, both CsA and anti-TNF- α agents downregulated IL-17A, IL-23p19, and chemokine (C-C motif) ligand 20 in psoriatic skin, thereby improving eruptions[42,44-46]. Collectively, these evidences suggest a strong involvement of IL-17A in the progression of psoriasis.

Interleukin-22 (IL-22) belongs to the IL-10 cytokine family[47-48] and is intimately linked to psoriatic inflammation (Fig. 1). It is primarily made by Th17 cells. However, T22 have also been shown to exclusively produce IL-22. The IL-22 receptor can be found on keratinocytes, wherein IL-22 stimulates epidermal hyperplasia via a rise in keratinocyte proliferation. Clinically, serum IL-22 is markedly elevated in psoriatic patients, as opposed to healthy individuals[49]. Additionally, IL-22 is known to be highly expressed in psoriatic lesions and the levels fall with anti-psoriatic therapy[39]. Based on these data, IL-22

not only plays a crucial role in keratinocyte proliferation, but also regulates psoriasis development and progression.

Dendritic cells produce interleukin (IL)-23, which regulates Th17 proliferation. The TH17 cells, in turn, are responsible for stimulating a variety of cytokines, including IL-17A, IL-17F, and IL-22. Among them, IL-17A and IL-22 was reported to be involved in keratinocyte proliferation and positively regulate tumor necrosis factor (TNF)- α , chemokine (C-X-C motif) ligand (CXCL)1, and CXCL8. Taken together, these conclusions suggest the involvement of these genes in multiple immune-provoked disease states.

Using single gene ROC analysis, we revealed that CXCL8 has great potential to serve as a bio-marker for psoriatic diagnosis (AUC values \approx 0.7). Moreover, based on CXCL8 predictions from starBase, miRDB and miRWalk, we generated a CXCL8-ceRNA network that included hsa-miR-1294, hsa-miR-140-3p, hsa-miR-185-5p, hsa-miR-4306, hsa-miR-4644, and hsa-miR-493-5p. lncRNAs modulate immune and inflammatory pathways via multi-mechanistic regulation of gene expression [50]. Among these mechanisms, the ceRNA axis has been widely investigated. Based on the ceRNA theory, lncRNA activates target gene expression by sequestering miRNA that would otherwise suppress gene activation. [51]. Qiao et. al. [52], for instance, revealed a lncRNA-MSX2P1 axis that stimulates S100A71 and facilitates IL-22-induced keratinocytes production via depressing miR-6731-5p action. Similarly, Li et al [53] reported that lncRNA H19 modulates keratinocyte differentiation by sequestering miR-130b-3p and augmenting desmoglein 1 expression. Consistent with these studies, our work also demonstrated a strong involvement of ceRNA in the development and progression of psoriasis via sequestering multiple potential miRNAs.

This study highlighted a promising bio-marker for psoriasis. Nevertheless, our work had some notable limitations. Firstly, the stratification analysis and interaction between factors did not receive detailed investigation. Moreover, due to its retrospective nature, we also couldn't rule out selective and recall biases. Hence, we propose prospective future studies to increase the statistical power and obtain more reliable conclusions. Secondly, apart from bioinformatics being a powerful tool for genome-wide studies, inadequate knowledge of underlying mechanisms may have limited our identification of effective psoriatic bio-markers. Hence, CXCL8 must be examined extensively at the molecular, cellular, and organismal level to confirm its significance in psoriatic diagnosis.

Conclusions

In summary, this study analyzed 265 psoriatic skin lesion samples to identify DEGs responsible for psoriasis progression. We revealed 197 total DEGs associated with psoriasis and we recognized CXCL8 as a key bio-marker for psoriasis. Further investigations are warranted to explore all aspects of CXCL8 function in psoriasis.

Abbreviations

GEO: Gene Expression Omnibus; DEGs: Differentially expressed genes;

GO: Gene ontology; KEGG: Kyoto Encyclopedia of Genes and Genomes;

PPI: Protein-protein interaction

Declarations

Acknowledgements

Not applicable.

Authors' contributions

YS designed the current study, performed data analysis and wrote the manuscript. ST and YY performed the literature review regarding cytokines in psoriasis. SX and JL analyzed the data. All authors read and approved the final manuscript.

Funding

This work was supported by the Program of Science and Technology Commission of Shanghai Municipality (No.18140901800)

Availability of data and materials

All data generated or analysed during this study are included in this published article.

Ethics approval and consent to participate

Not applicable.

Consent for publication

Not applicable.

Competing interests

The authors declare that they have no competing interests.

Authors' information

^a Department of Dermatology, Shanghai Skin Disease Hospital, School of medicine, Tongji University, Shanghai, 200443, China. ^b Institute of Psoriasis, School of medicine, Tongji University, Shanghai, 200092, China.

References

1. Nestle FO, Kaplan DH, Barker J. Psoriasis. *New Engl J Med* 361:496-509, 2009.

2. Jiang S, Hinchliffe TE, Wu T. Biomarkers of an auto immune skin disease-psoriasis. *Genom Proteom Bioinf* 13: 224-233, 2015.
3. Trowbridge RM, Pittelkow MR. Epigenetics in the pathogenesis and pathophysiology of psoriasis vulgaris. *J Drugs Dermatol* 13:111-118, 2014.
4. Brodmerkel C, Li K, Garcet S, et al. Modulation of inflammatory gene transcripts in psoriasis vulgaris: Differences between usteki-numab and etanercept. *J Allergy Clin Immunol* 143 (5): 1965-1969, 2019.
5. Ricceri F, Pescitelli L, Lazzeri L, et al. Clinical experience with infliximab biosimilar in psoriasis. *Br J Dermatol* 177 (6): e347-e348, 2017.
6. G.R. Burmester. K. B.Gordon. J. T. Rosenbaum, et al. Long-Term Safety of Adalimumab in 29,967 Adult Patients From Global Clinical Trials Across Multiple Indications: An Updated Analysis. *Adv. Ther* 37 (1): 364-380, 2020.
7. Carrascosa JM, Del-Alcazar E. New therapies versus first-generation biologic drugs in psoriasis: a review of adverse events and their management. *Expert Rev. Clin. Immu* 14 (4): 259-273, 2020.
8. Peranteau AJ, Turkeltaub AE, Tong Y, et al. A Review of Ixeki-zumab, an Anti-Interleukin-17A Monoclonal Antibody, for Moderate-to-Severe Plaque Psoriasis. *Skin Therapy Lett* 21(6): 1-6, 2016.
9. Feldman SR, Gomez B, Meng X, et al. Secukinumab rapidly improves EQ-5D health status in patients with psoriasis: Pooled analysis from four phase 3 trials. *J Dermatology Treat* 1-7, 2020.
10. Chen SC, de Groot M, Kinsley D, Lavery M, et al. Expression of chemokine receptor CXCR3 by lymphocytes and plasmacytoid dendritic cells in human psoriatic lesions. *Arch Dermatol Res* 302 (2): 113-23, 2010.
11. Pohl D, Andrys C, Borska L, et al. CC and CXC chemokines patterns in psoriasis determined by protein array method were influenced by Goeckerman's therapy. *Acta Medica* 52 (1): 9-13, 2009.
12. Christopherson K 2nd, Hromas R. Chemokine regulation of normal and pathologic immune responses. *Stem Cells* 19 (5): 388-396, 2001.
13. Ferrari SM, Ruffilli I, Colaci M, et al. CXCL10 in psoriasis. *Adv Med Sci* 60 (2): 349-354, 2015.
14. Nedoszytko B, Sokolowska-Wojdylo M, Ruckemann-Dziurdzinska K, et al. Chemokines and cytokines network in the pathogenesis of the inflammatory skin diseases: atopic dermatitis, psoriasis and skin mastocytosis. *Postepy Dermatol Alergol* 31 (2): 84-91, 2014.
15. Timoteo RP, Silva MV, Miguel CB, et al. Th1 /Th17-related cytokines and chemokines and their implications in the pathogenesis of pemphigus vulgaris. *Mediators Inflamm* 22(2): 715-1285, 2017
16. Helen H, Bikash D, Nouri N. Role of the CXCL8-CXCR1 /2 axis in cancer and inflammatory diseases. *Theranostics* 7(6) : 1543-1588, 2017
17. Barrett, T., et al., NCBI GEO: archive for functional genomics data sets—update. *Nucleic Acids Res* 41(Database issue): p. D991-5, 2013.
18. Liberzon A, Birger C, Thorvaldsdóttir H, Ghandi M, Mesirov JP, Tamayo P. The Molecular Signatures Database (MSigDB) hallmark gene set collection. *Cell Syst* Dec 23;1(6):417-425, 2015.

19. Goldman MJ, Craft B, Hastie M, Repečka K, McDade F, Kamath A, Banerjee A, Luo Y, Rogers D, Brooks AN, Zhu J, Haussler D. Visualizing and interpreting cancer genomics data via the Xena platform. *Nat Biotechnol* Jun 38(6): 675-678, 2020.
20. Gautier L, Cope L, Bolstad BM, Irizarry RA. *affy*—analysis of Affymetrix GeneChip data at the probe level. *Bioinformatics* 20(3): 307-15, 2004.
21. Ritchie ME, Phipson B, Wu D, Hu Y, Law CW, Shi W, Smyth GK. *limma* powers differential expression analyses for RNA-sequencing and microarray studies. *Nucleic Acids Res* Apr 20, 43(7): e47,2015.
22. Chen H, Boutros PC. *VennDiagram*: a package for the generation of highly-customizable Venn and Euler diagrams in R. *BMC Bioinformatics* Jan 26, 12: 35, 2011.
23. Russell CB, Rand H, Bigler J, Kerkof K, Timour M, Bautista E, Krueger JG, Salinger DH, Welcher AA and Martin DA : Gene expression profiles normalized in psoriatic skin by treatment with brodalumab, a human anti-IL- 17 receptor monoclonal antibody. *J Immunol* 192: 3828-3836, 2014.
24. Bigler J, Rand HA, Kerkof K, Timour M and Russell CB: Cross-study homogeneity of psoriasis gene expression in skin across a large expression range. *PLoS One* 8: e52242, 2013.
25. Yu G, Wang L-G, Han Y, He Q-Y. *clusterProfiler*: an R package for comparing biological themes among gene clusters. *OMICS: A Journal of Integrative Biology* 16(5): 284–287, 2012.
26. Subramanian A, Tamayo P, Mootha VK, Mukherjee S, Ebert BL, Gillette MA, Paulovich A, Pomeroy SL, Golub TR, Lander ES, Mesirov JP. Gene set enrichment analysis: a knowledge-based approach for interpreting genome-wide expression profiles. *Proceedings of the National Academy of Sciences of the United States of America* 102(43): 15545–15550, 2005.
27. Von Mering, C., et al. *STRING*: a database of predicted functional associations between proteins. *Nucleic Acids Res* 31(1): p. 258-61, 2003.
28. Shannon, P., et al. *Cytoscape*: a software environment for integrated models of biomolecular interaction networks. *Genome Res* 13(11): p. 2498-504, 2003.
29. Ito, K. and D. Murphy. Application of *ggplot2* to Pharmacometric Graphics. *CPT Pharmacometrics Syst Pharmacol* 2: p. e79, 2013.
30. Chen, B., et al. Profiling Tumor Infiltrating Immune Cells with *CIBERSORT*. *Methods Mol Biol* 1711: p. 243-259, 2018.
31. Akobeng AK. Understanding diagnostic tests 3: receiver operating characteristic curves. *Acta Paediatrica* 96(5): 644–647, 2007.
32. Robin X, Turck N, Hainard A, Tiberti N, Lisacek F, Sanchez J-C, Müller M. *pROC*: an open-source package for R and S+ to analyze and compare ROC curves. *BMC Bioinformatics* 12(1): 77, 2011.
33. Jeggari A, Marks DS, Larsson E. *miRcode*: a map of putative microRNA target sites in the long non-coding transcriptome. *Bioinformatics* 28(15): 2062–2063, 2012.
34. Li, J.H., et al. *starBase v2.0*: decoding miRNA-ceRNA, miRNA-ncRNA and protein-RNA interaction networks from large-scale CLIP-Seq data. *Nucleic Acids Res* 42(Database issue): p. D92-7, 2014.

35. Chen, Y. and X. Wang, miRDB: an online database for prediction of functional microRNA targets. *Nucleic Acids Res* 48 p. D127-D131, 2020.
36. Dweep, H., N. Gretz, and C. Sticht, miRWalk database for miRNA-target interactions. *Methods Mol Biol* 1182: p. 289-305, 2014.
37. Uhlen, M., et al. Proteomics. Tissue-based map of the human proteome. *Science* 347(6220): p. 1260419, 2015.
38. Valent F, Tullio A, Errichetti E, Stinco G. The epidemiology of psoriasis in an Italian area: population-based analysis of administrative data. *G Ital Dermatol Venereol* 29 (6) : Epub ahead of print, 2018.
39. Krueger G, Koo J, Lebwohl M, et al. The impact of psoriasis on quality of life: results of a 1998 National Psoriasis Foundation patient-membership survey. *Arch Dermatol* 137 (3) : 280-284, 2001.
40. ARTUC M, GUHL S, BABINA M, et al. Mast cell-derived TNF-alpha and histamine modify IL-6 and IL-8 expression and release from cutaneous tumor cells. *Exp Dermatol* 20(12): 1020-1022, 2011.
41. Teunissen MBM, Koomen CW, De Waal Malefyt R, Wierenga EA, Bos JD. Interleukin-17 and interferon-gamma synergize in the enhancement of proinflammatory cytokine production by human keratinocytes. *J Invest Dermatol* 111: 645-649, 1998.
42. Lowes MA, Kikuchi T, Fuentes-Duculan J et al. Psoriasis vulgaris lesions contain discrete populations of Th1 and Th17 T cells. *J Invest Dermatol* 128: 1207-1211, 2008.
43. Van der Fits L, Mourits S, Voerman JS et al. Imiquimod-induced psoriasis-like skin inflammation in mice is mediated via the IL-23/IL-17 axis. *J Immunol* 182: 5836-5845, 2009.
44. Zaba LC, Cardinale I, Gilleaudeau P et al. Amelioration of epidermal hyperplasia by TNF inhibition is associated with reduced Th17 responses. *J Exp Med* 204: 3183-3194, 2007.
45. Haider AS, Cohen J, Fei J et al. Insights into gene modulation by therapeutic TNF and IFN gamma antibodies: TNF regulates IFN gamma production by T cells and TNF-regulated genes linked to psoriasis transcriptome. *J Invest Dermatol* 128: 655-666, 2008.
46. Haider AS, Lowes MA, Suarez-Villa M et al. Identification of cellular pathways of "type 1," Th17 T cells, and TNF- and inducible nitric oxide synthase-producing dendritic cells in auto-immune inflammation through pharmacogenomic study of cyclosporine A in psoriasis. *J Immunol* 180: 1913-1920, 2008.
47. Sonnenberg GF, Fouser LA, Artis D. Border patrol: regulation of immunity, inflammation and tissue homeostasis at barrier surfaces by IL-22. *Nat Immunol* 12: 383-390, 2011.
48. Fujita H. The role of IL-22 and Th22 cells in human skin diseases. *J Dermatol Sci* 72: 3-8, 2013.
49. Wolk K, Witte E, Wallace E et al. IL-22 regulates the expression of genes responsible for antimicrobial defense, cellular differentiation, and mobility in keratinocytes: a potential role in psoriasis. *Eur J Immunol* 36: 1309-1323, 2006.
50. Wu GC, Pan HF, Leng RX, Wang DG, Li XP, Li XM and Ye DQ: Emerging role of long noncoding RNAs in autoimmune diseases. *Auto immune Rev* 14: 798-805, 2015.

51. Tay Y, Rinn J, Pandolfi PP. The multilayered complexity of ceRNA crosstalk and competition. *Nature* 505: 344-352, 2014.
52. Qiao M, Li R, Zhao X, Yan J and Sun Q: Up-regulated lncRNA-MSX2P1 promotes the growth of IL-22-stimulated keratinocytes by inhibiting miR-6731-5p and activating S100A7. *Exp Cell Res* 363: 243-254, 2018.
53. Li CX, Li HG, Huang LT, Kong YW, Chen FY, Liang JY, Yu H and Yao ZR: H19 lncRNA regulates keratinocyte differentiation by targeting miR-130b-3p. *Cell Death Dis* 8: e3174, 2017.

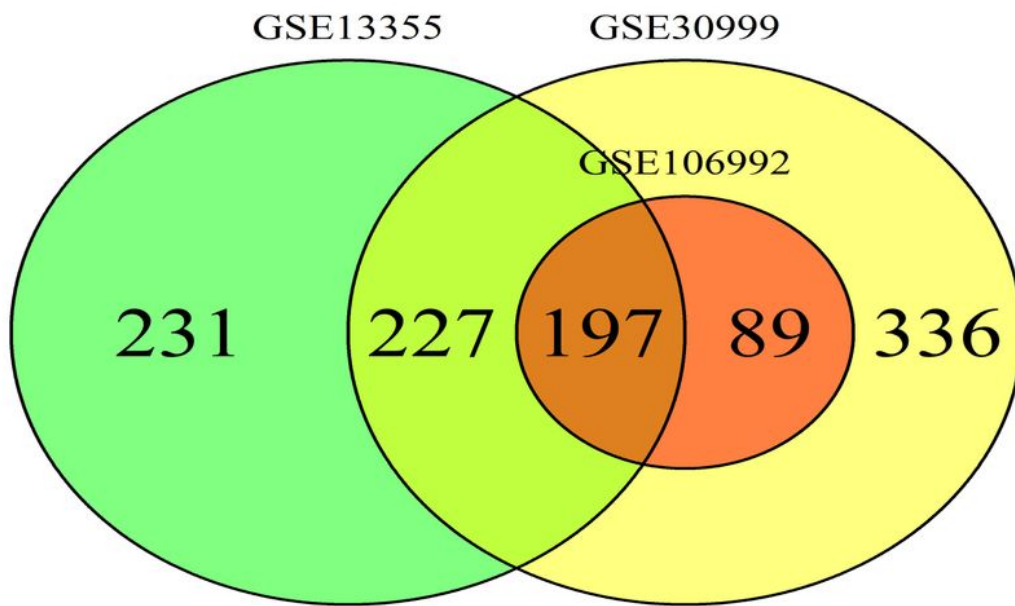
Tables

Table1. GO and KEGG pathway enrichment analysis of DEGS in psoriasis samples.

GO-BP		
ID	Description	p.adjust
GO:0051607	defense response to virus	P<0.001
GO:0009615	response to virus	P<0.001
GO:0060337	type I interferon signaling pathway	P<0.001
GO:0071357	cellular response to type I interferon	P<0.001
GO:0034340	response to type I interferon	P<0.001
GO-CC		
ID	Description	p.adjust
GO:0001533	cornified envelope	P<0.001
GO:0034774	chromosomal regionsecretory granule lumen	P<0.001
GO:0060205	cytoplasmic vesicle lumen	P<0.001
GO:0031983	vesicle lumen	P<0.001
GO:0035580	specific granule lumen	P<0.001
GO-MF		
ID	Description	p.adjust
GO:0042379	chemokine receptor binding	P<0.001
GO:0004252	serine-type endopeptidase activity	P<0.001
GO:0005125	cytokine activity	P<0.001
GO:0005126	cytokine receptor binding	P<0.001
GO:0048020	CCR chemokine receptor binding	P<0.001
KEGG		
ID	Description	p.adjust
hsa04657	IL-17 signaling pathway	P<0.001
hsa04061	Viral protein interaction with cytokine and cytokine receptor	P<0.001
hsa04621	NOD-like receptor signaling pathway	P<0.001
hsa00983	Drug metabolism - other enzymes	0.0018
hsa05160	Hepatitis C	0.0028

Figures

A



B

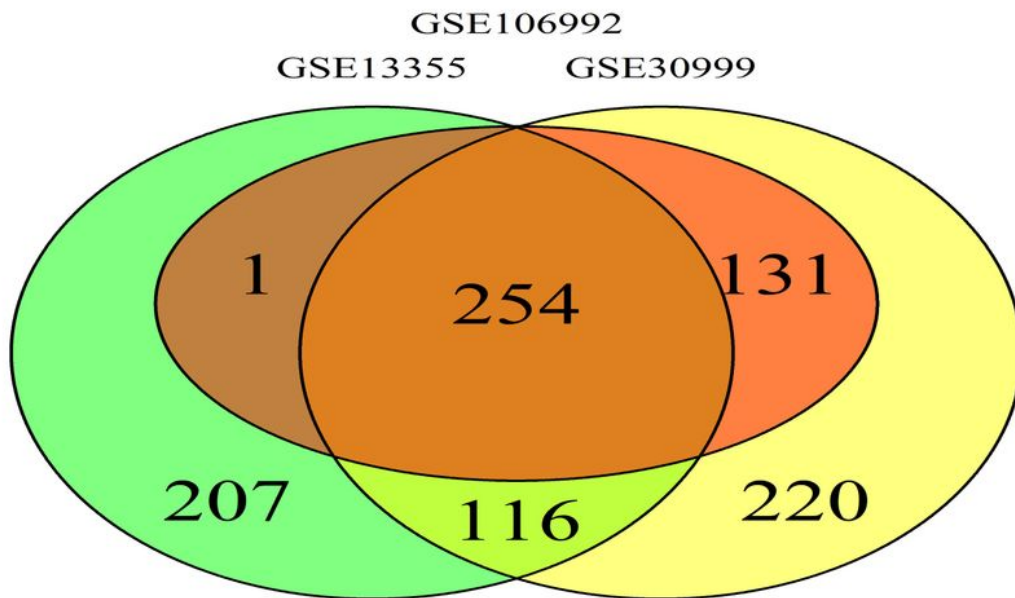
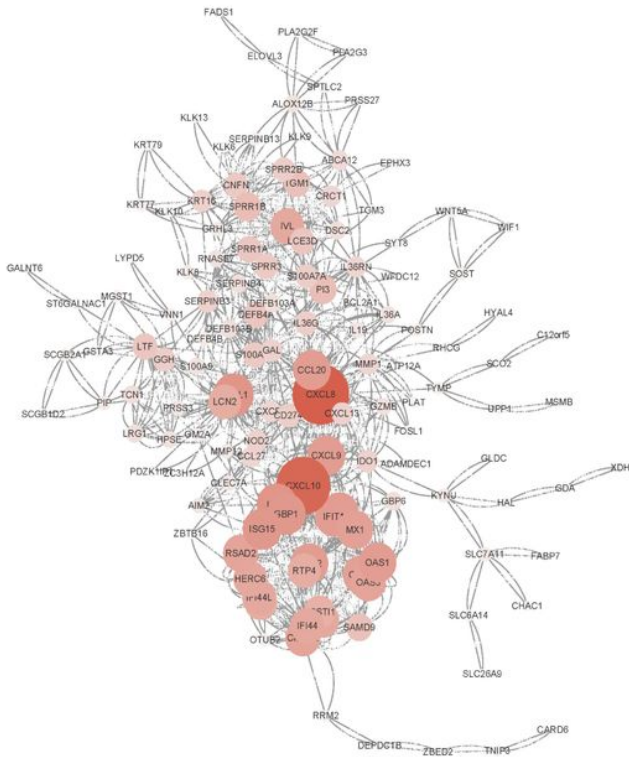


Figure 1

(A) Venn Diagram DEGs in both psoriatic and NN skin group. (B) Venn Diagram DEGs in both high-expression and low-expression group. The intersection part represents the shared DEGs between both groups.

A



B

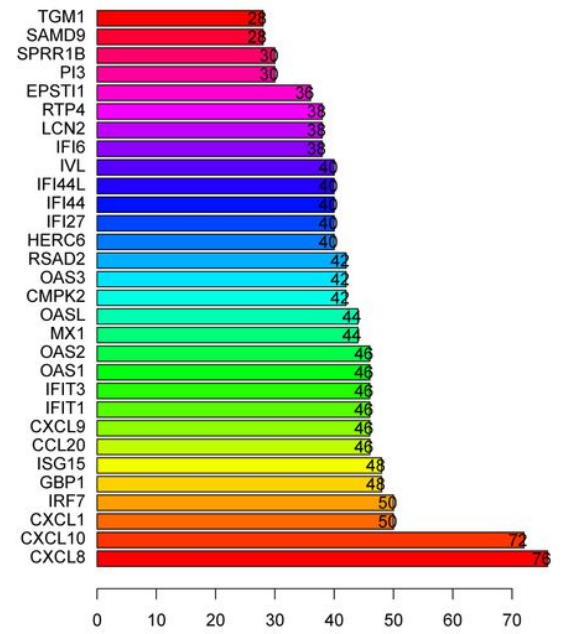


Figure 2

(A) PPI network and the most significant module of DEGs. (B) Degree distribution of 197 DEGs.

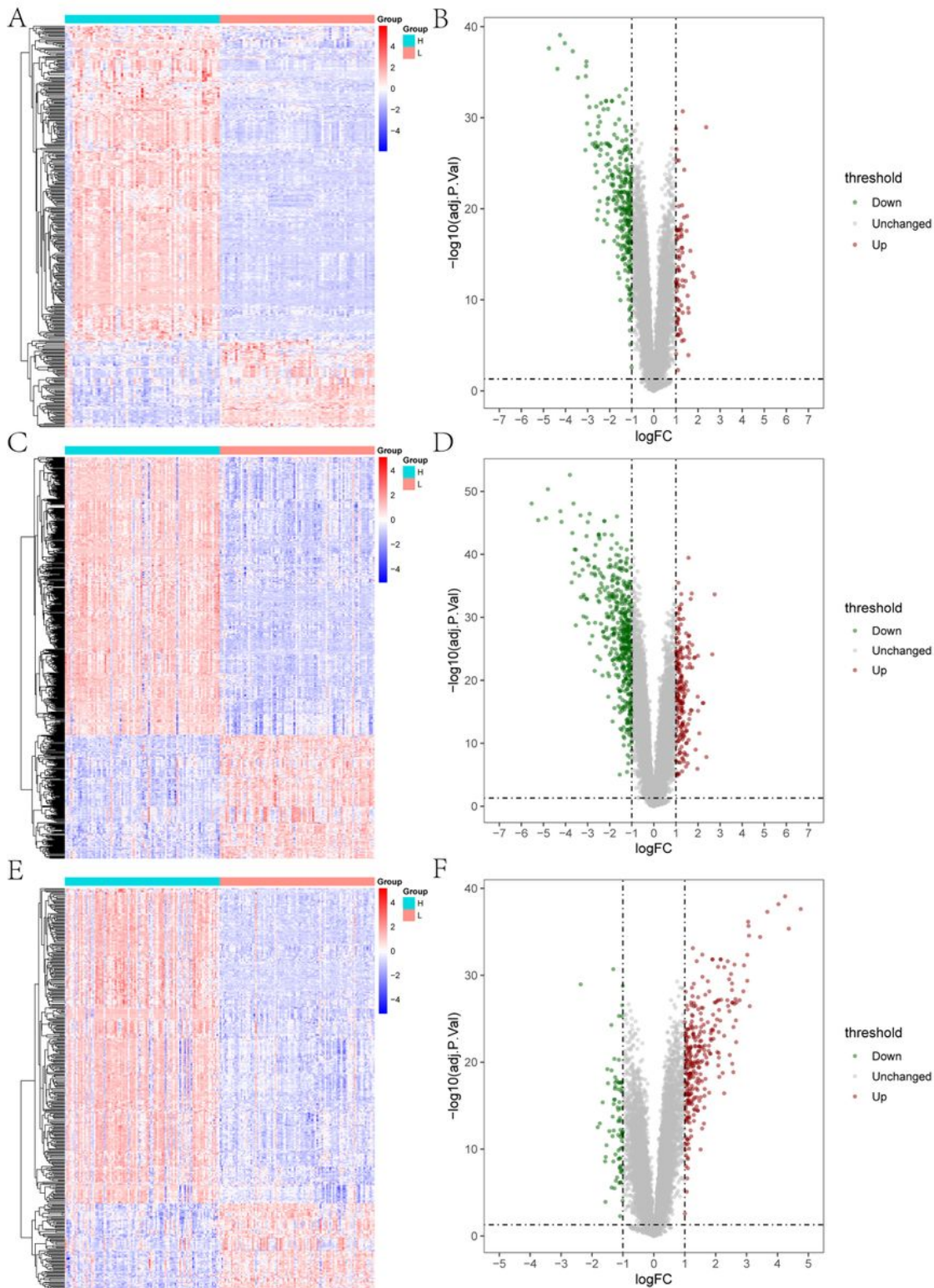


Figure 3

GSE13355, GSE30999 and GSE106992 were divided into high and low expression groups. The distribution density map and the principal component analysis between the two groups were shown. (A) GSE13355 distribution density map. (B) GSE30999 distribution density map. (C) GSE106992 distribution density map. (D) GSE13355 principal component analysis. (E) GSE30999 principal component analysis. (F) GSE 106992 principal component analysis.

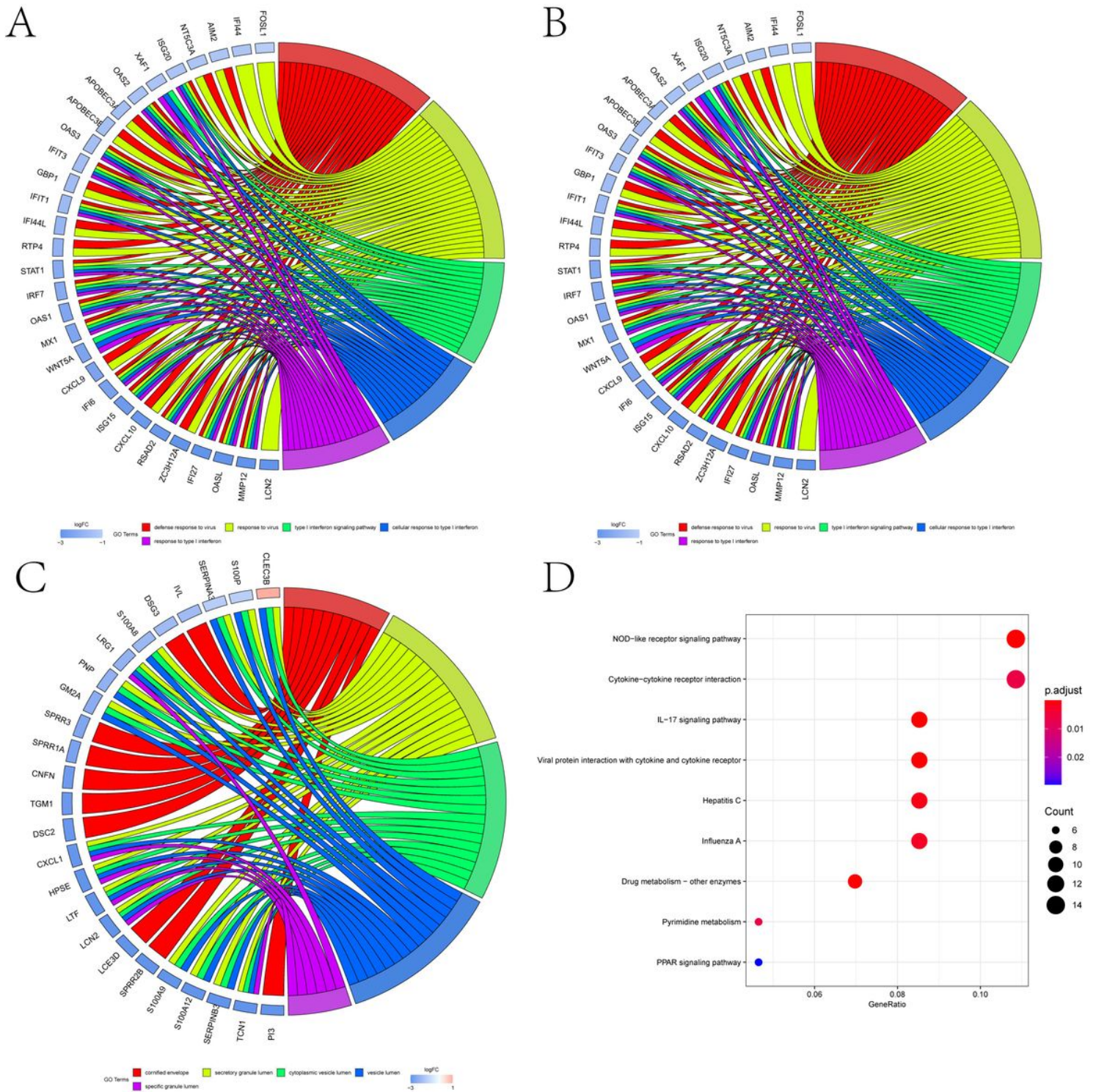


Figure 4

GO and KEGG pathway enrichment analysis of CXCL8 in psoriasis samples. (A) GO-BP (B) GO-MF (C) GO-CC (D) KEGG

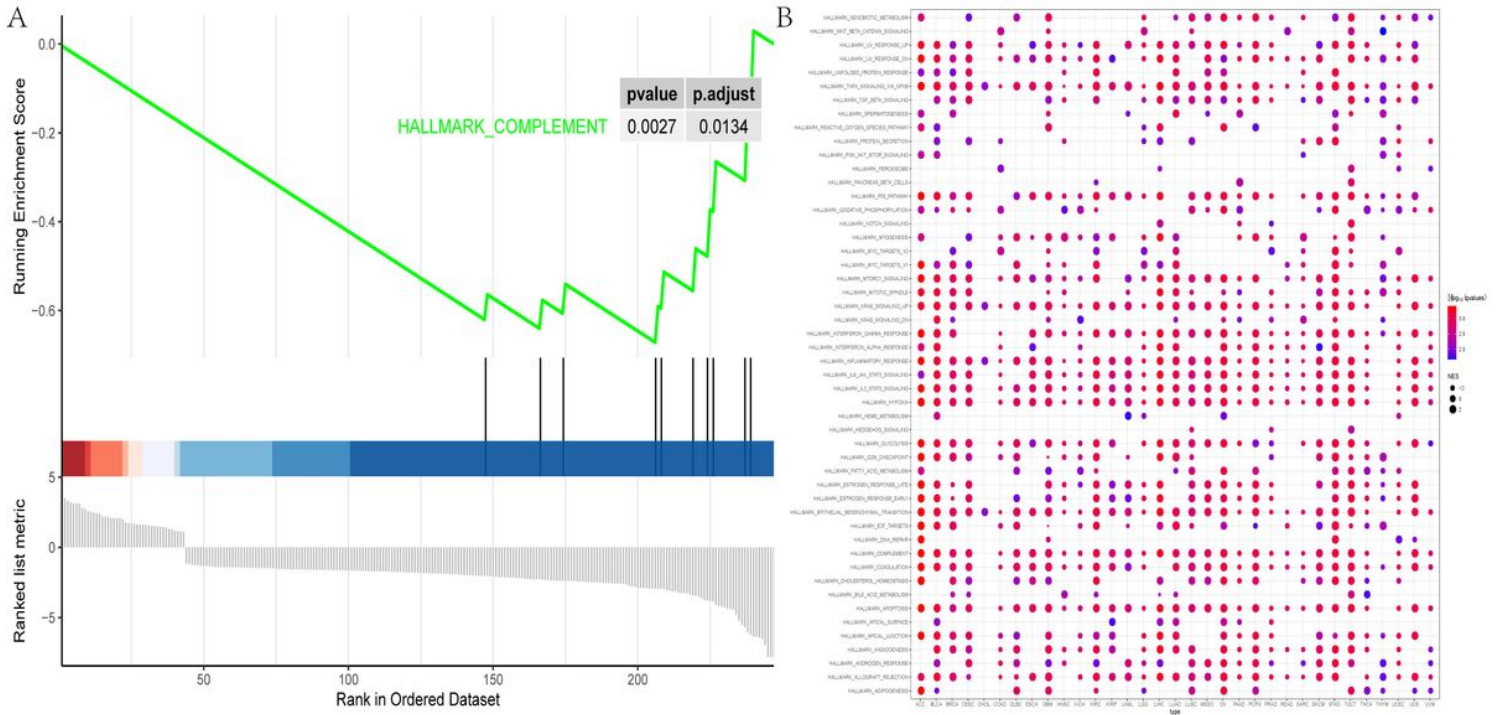
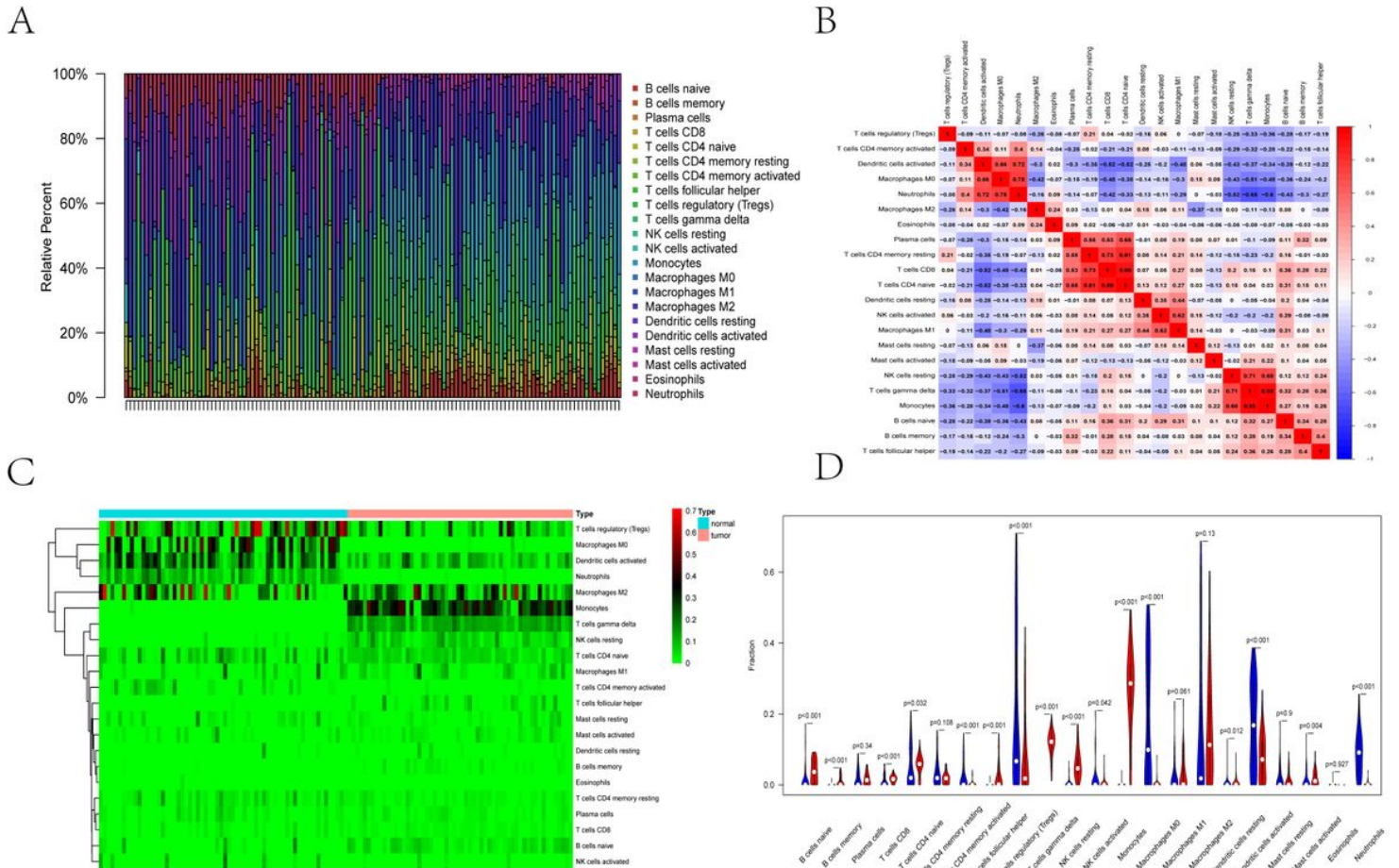


Figure 5

(A) GSEA analysis of CXCL8. (B) Pan-cancer pathway of CXCL8.



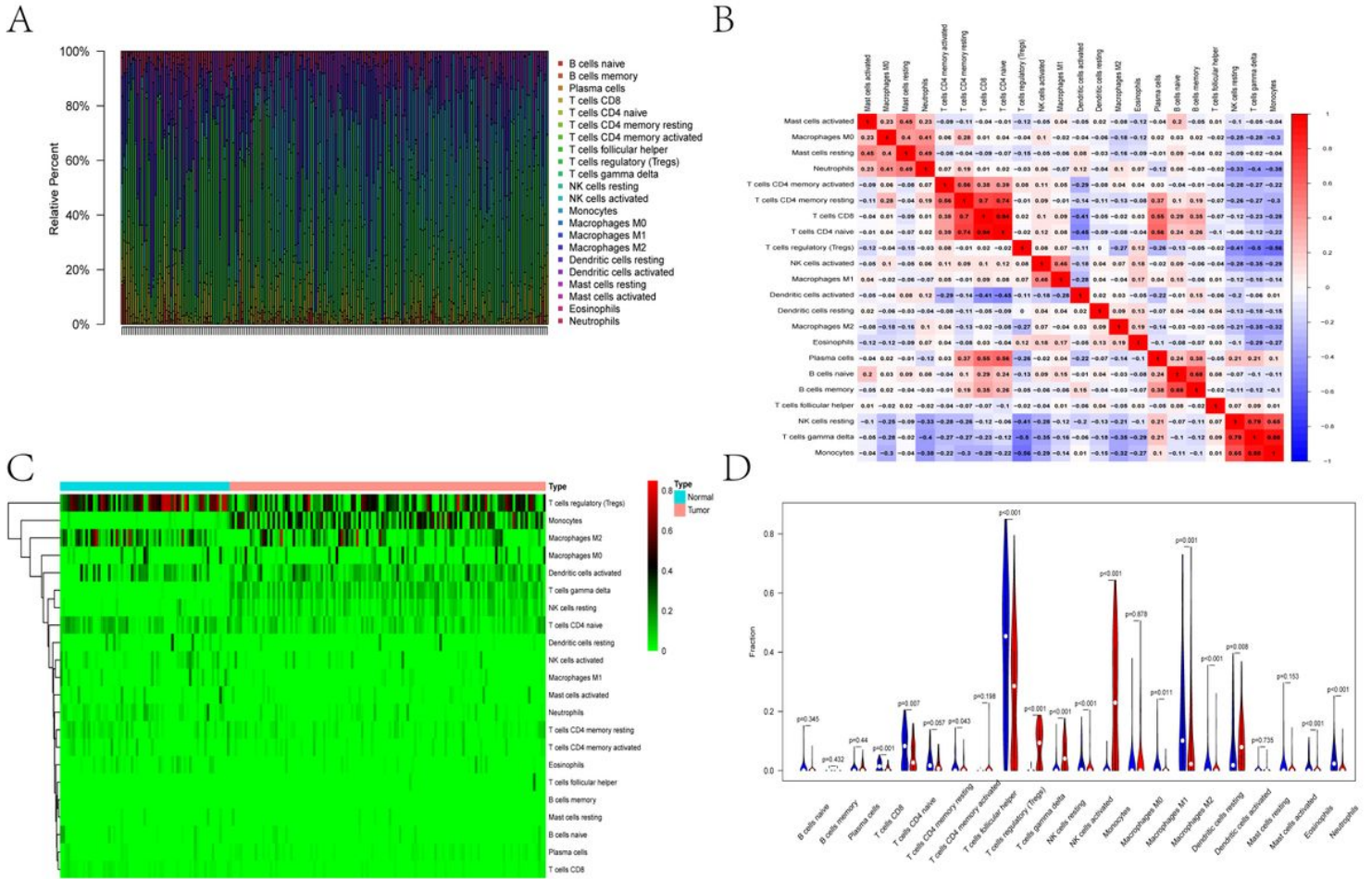


Figure 8

Immune infiltration analysis in GSE106992. (A) Immune cell analysis was shown in the bar graph. (B) The correlation of the expression of immune cells was analyzed. (C) The difference in the expression of immune cells between disease and normal samples was analyzed, as shown in the heat map. (D) The difference in the expression of immune cells between disease and normal samples was analyzed, as shown in the violin plot.

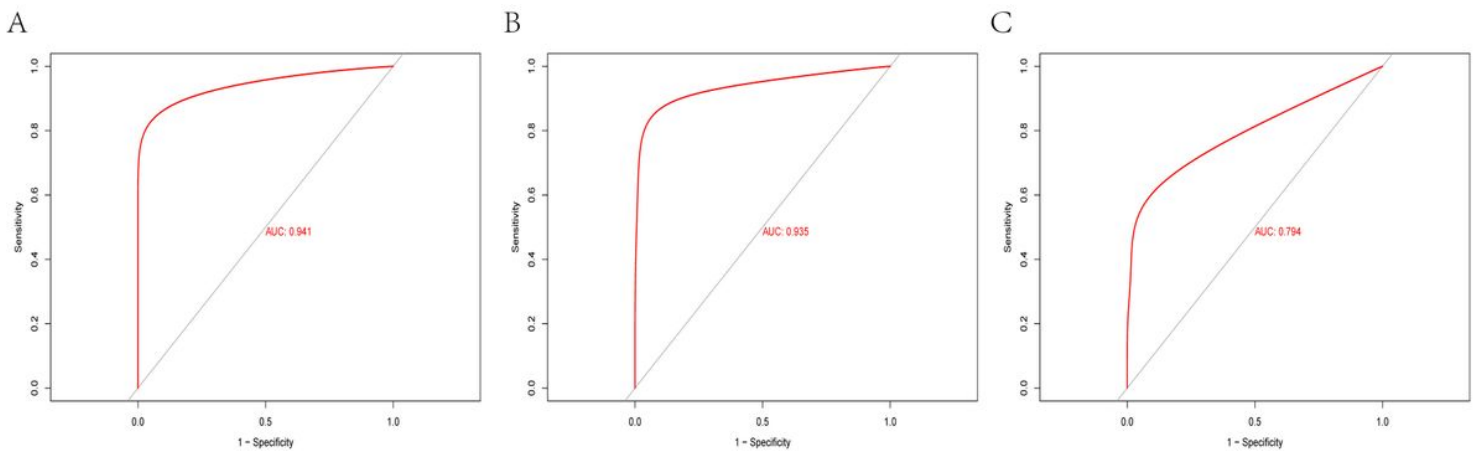


Figure 9

ROC curve analysis of CXCL8 in three datasets. (A) The area under the ROC curve was 0.941 for GSE13355. (B) The area under the ROC curve was 0.935 for GSE30999. (C) The area under the ROC curve was 0.794 for GSE106992.

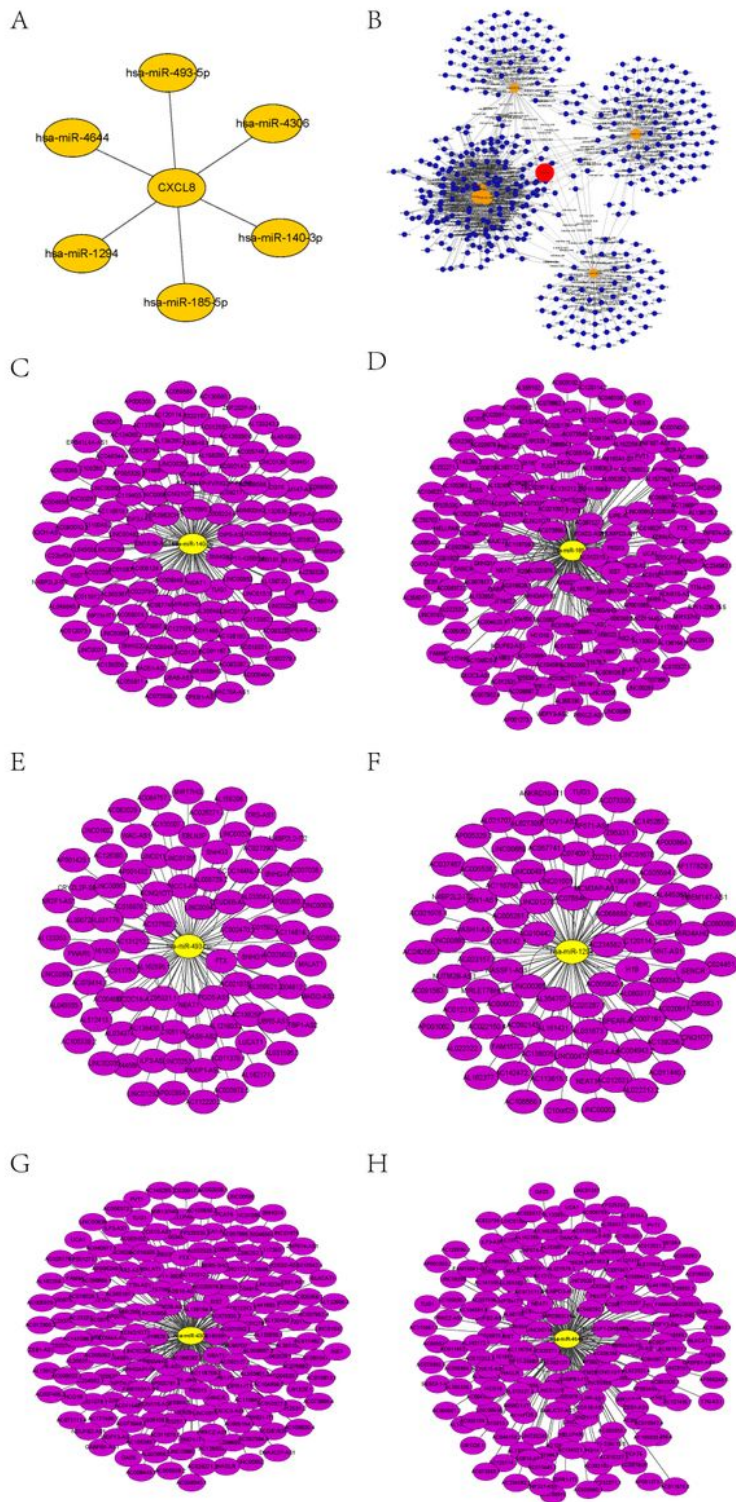


Figure 10

(A) Interactive network of CXCL8-miRNA. (B) CeRNA network of CXCL8-miRNA-LncRNA. (C-H) Six interactive networks of miRNA-LncRNA.

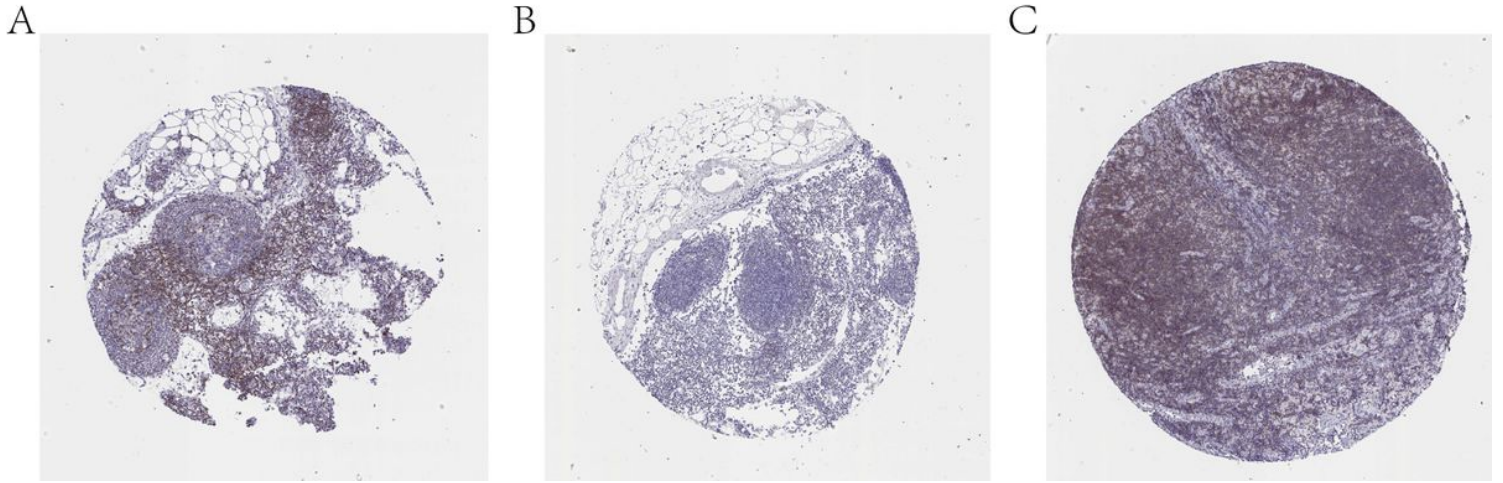


Figure 11

Immunohistochemical study on lymph node of CXCL8.